REPORT DOCUMENTATION PAGE

Form Approved
OMB NO. 0704-0188

1. AGENCY USE ONLY (Leave Blank)	2. REPORT DATE 3/29/02	3. REPORT TYPE AND DATES COVERED Final Progress Report 7/1/98-12/31/01

4. TITLE AND SUBTITLE
Plasma Based Devices

5. FUNDING NUMBERS
DAAG 55-98-1-0408

6. AUTHOR(S)
M. Gundersen

7. PERFORMING ORGANIZATION NAME(S) AND ADDRESS(ES)
University of Southern California
Dept. of Electrical Engineering-Electrophysics
Los Angeles, CA 90089-0271 213-740-7874

8. PERFORMING ORGANIZATION REPORT NUMBER

9. SPONSORING / MONITORING AGENCY NAME(S) AND ADDRESS(ES)

U. S. Army Research Office
P.O. Box 12211
Research Triangle Park, NC 27709-2211

10. SPONSORING / MONITORING AGENCY REPORT NUMBER

38947.4-PH

11. SUPPLEMENTARY NOTES

The views, opinions and/or findings contained in this report are those of the author(s) and should not be construed as an official Department of the Army position, policy or decision, unless so designated by other documentation.

12 a. DISTRIBUTION / AVAILABILITY STATEMENT

Approved for public release; distribution unlimited.

12 b. DISTRIBUTION CODE

13. ABSTRACT (Maximum 200 words)

Please see attached.

14. SUBJECT TERMS

15. NUMBER OF PAGES
28

16. PRICE CODE

17. SECURITY CLASSIFICATION OR REPORT	18. SECURITY CLASSIFICATION ON THIS PAGE	19. SECURITY CLASSIFICATION OF ABSTRACT	20. LIMITATION OF ABSTRACT
UNCLASSIFIED	UNCLASSIFIED	UNCLASSIFIED	UL

MASTER COPY: PLEASE KEEP THIS "MEMORANDUM OF TRANSMITTAL" BLANK FOR REPRODUCTION PURPOSES. WHEN REPORTS ARE GENERATED UNDER THE ARO SPONSORSHIP, FORWARD A COMPLETED COPY OF THIS FORM WITH EACH REPORT SHIPMENT TO THE ARO. THIS WILL ASSURE PROPER IDENTIFICATION. NOT TO BE USED FOR INTERIM PROGRESS REPORTS; SEE PAGE 2 FOR INTERIM PROGRESS REPORT INSTRUCTIONS.

MEMORANDUM OF TRANSMITTAL

U.S. Army Research Office
ATTN: AMSRL-RO-BI (TR)
P.O. Box 12211
Research Triangle Park, NC 27709-2211

☐ Reprint (Orig + 2 copies)

☐ Technical Report (Orig + 2 copies)

☐ Manuscript (1 copy)

☒ Final Progress Report (Orig. + 2 copies)

☐ Related Materials, Abstracts, Theses (1 copy)

CONTRACT/GRANT NUMBER: DAAG 55-98-1-0408

REPORT TITLE: Plasma Based Devices

is forwarded for your information.

SUBMITTED FOR PUBLICATION TO (applicable only if report is manuscript):

Sincerely,

Martin Gundersen

PLASMA BASED DEVICES

FINAL PROGRESS REPORT

M. GUNDERSEN

DECEMBER 2001

U. S. ARMY RESEARCH OFFICE

GRANT NO: DAAG55-98-1-0408

APPROVED FOR PUBLIC RELEASE;

DISTRIBUTION UNLIMITED

TABLE OF CONTENTS

STATEMENT OF THE PROBLEM STUDIED

Plasma processing is now considered an exciting prospect for control of noxious effluents from many different sources including diesel engines, power plants, factories, and incinerators. Energy-efficient plasma-based technologies, supported through this grant, are now under commercial investigation for pollution abatement, and have potential for reduced emissions, higher efficiencies, simplified processing, and lower costs, while allowing the use of existing power plants and energy sources. Such advances are critically important to the maintenance of a competitive industrial infrastructure while simultaneously reducing pollutants, greenhouse gases and energy usage. Successful plasma systems for emissions control will, for example, allow continued use of energy-efficient diesel engines in moving and stationary sources, and can be detached under emergency DOD conditions. One attaches a plasma "muffler" to provide a plasma chemistry that takes advantage of significantly enhanced plasma-chemical processes through increased rates and related cross-sections of interactions between species which reduces emissions. Research supported by the ARO at USC has developed new plasma technology for remediation of nitrogen oxides (NO_x) sources including diesel engines. In work to date, we have found efficient, effective NOx reduction using pulsed power techniques.

This method will have broad and very significant impact on the reduction of other forms of air pollution. This technology will, in our judgment, also allow plasma treatment of volumes of combustive fuel by ion and radical injection at low energy cost, thus enhancing combustion, reducing emissions and signatures, and holding promise for leaner-burning combustants, all of which are important for the DOD.

The most promising methods are based on applications of transient plasmas and on advanced power conditioning. Transient plasmas are highly non-equilibrium and initiate key processes — particularly affecting excited state, ion, and radical populations — during a few nsec. Key questions included the level of sophistication that is required for implementation and operation, and the energy efficiency that can be obtained by such a device.

This research integrated addressed promising concepts and basic issues, tightly coupling modulator design, advanced diagnostics, and exploration of new applications. The study of **transient plasmas**, and the enabling pulsed power technology, led to new directions in the areas of **ignition**, and biological applications of short-pulse technology, of the technology.

The report describes 3 areas for results. In addition to new directions in emissions studies, the initial results on ignition, and biological applications of the pulsed power technology are reported.

SUMMARY OF THE MOST IMPORTANT RESULTS

Pollution: TCE Results

We studied the role and effect of oxygen concentration on the energy required for transient plasma destruction of trichloroethylene (TCE) over a wide range of initial TCE concentrations (100-2500 ppm). Optimal conditions for oxygen content and water vapor have been identified. The optimum oxygen concentration depends approximately linearly on the initial TCE concentration; however, the effect of oxygen content on the decomposition process is quite different for low (hundreds ppm) and high (thousands ppm) initial concentrations. For low concentrations the removal efficiency requires less energy in pure nitrogen than at standard atmospheric conditions (20% O_2); however, at high concentrations decomposition in pure N_2 requires significantly more energy than with O_2 present. Further, at higher concentrations in pure N_2 the removal efficiency does not depend exponentially on energy input. This result, an analysis of byproducts, and studies of NO added to the flow indicates that reactions with N radicals rather then electron attachment are responsible for the major contribution to remediation at high concentration in pure N_2.

The chemistry of TCE decomposition in gas mixtures containing oxygen is quite complicated, including hundreds of reactions with many intermediate byproducts. For many reactions there is no experimental data for reactions rates. These experiments, supported by the ARO, demonstrate that there is qualitative difference in the decomposition process for the low and high TCE concentrations, and this investigation provides a set of experimental data for cold plasma TCE decomposition for a broad range of the initial concentrations that are appropriate for many practical and research situations. Optimal conditions for oxygen content and water vapor have been identified. Additional details are included as Appendix I.

Ignition: Reduction of Delay to Combustion with Transient Plasma

Under ARO support we conducted an extensive observation of flame ignition by pulsed corona discharge, trying to learn the fundamental corona ignition phenomena, understand underlying physics and compare them with conventional spark plug ignition to determine whether a **transient discharge, sometimes termed pulsed corona or corona** discharge is a promising way to ignite flame. The observations include: combustion performances (pressure rise time, delay time, peak pressure and residual pressure.) of various fuels, pressure effects and performances of various electrodes. Five fuels were investigated: methane, propane, n-butane, iso-butane and octane.

A pulsed corona discharge is the transient phase of electric discharge before arc formation, and differs from conventional spark discharges in that the pulsed corona discharge has (1) spatially

more extensive distribution of plasma species than typical sparks; (2) higher fractions of electron energies which match electron excitation cross sections for dissociation and ionization energies of molecules; (3) higher energy efficiency and (4) the possibility of in-situ NOx destruction. This paper reports experimental investigations of pulsed corona ignition using various fuels including methane, propane, iso-butane, n-butane and iso-octane at both high (>1 atm.) and low (<1 atm.) pressure regions with varying electrode structures. Experimental results show that compared with conventional spark ignition, flame ignited with pulsed corona discharges have faster (**typically by a factor of 3**) pressure rise time, shorter delay time, higher maximum pressure and more complete combustion. Potential applications include improving thermal efficiency and lowering pollutant emission of internal combustion engines, high altitude relight of jet engines, flame holding in high-velocity jets. Additional details are included as Appendix II.

The Application of Pulsed Power to Intra-cell Biological Systems

Selective modification of intracellular proteomic processes without damage to external or internal membranes, irreversible pore formation or other irreversible effects on cell organelles is desirable for the development of therapeutic treatment of genetic and proteomic disorders, and is needed for studies of intracellular biochemistry, caspase activation, gene functions, and other basic cellular processes. It was found that electric fields (of the order 20 kV/cm averaged within cuvettes) persisting 20 nsec, applied repetitively (typ. 8–50 pulses) and without direct cell-electrode contact perturb internal cellular membranes and the compartmentalized intracellular environment without permanent damage. Additional details will be provided in the first report for the ARO renewal grant.

LIST OF MANUSCRIPTS SUBMITTED OR PUBLISHED UNDER ARO SPONSORSHIP

Papers published in peer-reviewed journals

"Plasma processing of diesel exhaust by pulsed corona discharge," V. Puchkarev, G. Roth, and M. Gundersen, 1998 SAE International Fall Fuels and Lubricants Meeting, San Francisco, CA, October 19-22, 1998.

"Laser-induced fluorescence images of NO distribution after needle-plane pulsed negative corona discharge," G. J. Roth and M. A. Gundersen IEEE Trans. Plasma Sci. **27**, 28 (1999).

"High power switches," M. Gundersen and G. Roth, in "The Handbook of Accelerator Physics and Engineering," Eds. A. Chao and Maury Tigner, World Scientific Publishing Co. (1999).

Book Chapter: "Transient Plasma-Assisted Diesel Exhaust Remediation, M. Gundersen, V. Puchkarev, A. Kharlov, G. Roth, J. Yampolsky and D. Erwin, submitted for inclusion in "Lectures in Plasma Physics and Plasma Technology", to be published by Wiley-Verlag Chemie.

Papers published in non-peer-reviewed journals or in conference proceedings

"Application of pulsed corona discharge to diesel exhaust remediation," V. Puchkarev, A. Kharlov and M. Gundersen, Proceedings of the 12th IEEE Pulsed Power Conference, Monterey, CA June 27-30, 1999.

"Energy efficient plasma treatment of diesel emission using a short pulse discharge: Physics and applications," V. Puchkarev, G. Roth and M. Gundersen University of Southern California, Los Angeles CA, Proceedings of the DEER Conference, Castine, ME, July 6, 1998.

"Plasma processing of diesel exhaust by pulsed corona discharge," Victor Puchkarev, Gregory J. Roth, and Martin Gundersen, Proceedings of the 11th ONR Propulsion Program Contractors Meeting, Palm Beach, FL, August 17-19, 1998.

"Laser induced fluorescence study of Nox in streamer discharge," A. Kharlov, G. Roth, V. Puchkarev and M. Gundersen, IEEE ICOPS '99, Monterey, CA June 24-28, 1999.

"Results from the ONR-ESS study at USC of plasma-assisted diesel exhaust remediation," M. Gundersen, V. Puchkarev, A. Kharlov, G. Roth, J. Yampolsky, and D. Erwin, Proceedings of the 12th ONR Propulsion Program Contractors Meeting, Salt Lake City, UT, August 3-6, 1999.

Manuscripts submitted, but not published

"Transient Plasma Decomposition of Trichloroethylene: Contrasting Roles for Oxygen and Nitrogen in Energy Cost Minimization", A. Kharlov and M.A. Gundersen, Appl. Phys. Lett. (Submitted)

Technical reports submitted to ARO
M. Gundersen, Interim Progress Report, December 1998
M. Gundersen, Interim Progress Report, December 1999

LIST OF PARTICIPATING SCIENTIFIC PERSONNEL:

M. Gundersen
J. Yampolsky
J.B. Liu
M. Behrend
X. Gu
C. Young
A. Kuthi
A. Ghalam

REPORT OF INVENTIONS (BY TITLE ONLY):

Pollution treatment cells energized by short pulses repetitive power pulse generator with fast rising pulse (USC File # 2570 & 2956)

BIBLIOGRAPHY

APPENDIXES

Appendix I: O_2 content and the pulsed corona decomposition of trichloroethylene

Appendix 2: Premixed flame ignition by pulsed transient plasma, or corona

TECHNOLOGY TRANSFER

The research produced potential technology transfer results in the areas of pulsed power, ignition, and the biological applications of pulsed power, as well as the pollution emission reduction. Several patent applications have been filed, and nondisclosure agreements have been entered into with several companies. Some of the interest, for commercial applications, is proprietary. The level of interest has reduced the rate of rapid publication, however, it is anticipated that all research supported by the ARO will continue to be published.

The pollution control approach using repetitive pulsed power is under investigation by engine, automobile, and electronic manufacturers. Typical companies include Ford Motor Company, Delphi Electronics, and Detroit Diesel Corporation. The value of intellectual property generated at USC (that is, the amount of patent protection for commercial applications) under the grant is not clear at this time.

Patents have been applied for in pulsed power technology, ignition using transient plasmas, and biological applications. The ARO will be advised as the technology transfer of these progresses.

Appendix I: O_2 content and the pulsed corona decomposition of trichloroethylene

Reported here are studies of the role and effect of oxygen concentration on the energy required for transient plasma destruction of trichloroethylene (TCE) over a wide range of initial TCE concentrations (100-2500 ppm). Optimal conditions for oxygen content and water vapor have been identified. The optimum oxygen concentration depends approximately linearly on the initial TCE concentration; however, the effect of oxygen content on the decomposition process is quite different for low (hundreds ppm) and high (thousands ppm) initial concentrations. For low concentrations the removal efficiency requires less energy in pure nitrogen than at standard atmospheric conditions (20% O_2); however, at high concentrations decomposition in pure N_2 requires significantly more energy than with O_2 present. Further, at higher concentrations in pure N_2 the removal efficiency does not depend exponentially on energy input. This result, an analysis of byproducts, and studies of NO added to the flow indicates that reactions with N radicals rather then electron attachment are responsible for the major contribution to remediation at high concentration in pure N_2. A brief discussion of the reaction chemistry and possible mechanisms, and the influence of humidity, is presented.

I Introduction

Energy requirements for plasma decomposition of gaseous pollutants such as trichloroethylene (C_2HCl_3, or TCE) will limit useful applications of the various forms of plasma technology for emissions abatement and remediation, and it is essential that energy efficient approaches be developed and understood for these approaches to be practical. In addition, energy required varies as a function of pollutant concentration, so that an additional requirement is the need for energy efficiency over a range of concentrations. In particular, scaling of energy as a function of concentration must be understood for successful implementation, and for an understanding of the underlying physics.

TCE is a common industrial solvent, regarded as hazardous and carcinogenic, whose entry into the environment must be reduced. Methods for TCE removal from gas streams include absorption, condensation, thermal incineration and catalytic removal. Pulsed plasma methods have potential advantages for concentrations as low as or lower than a few thousand ppm relative to these other methods, and plasma reactors using corona discharges are not susceptible to poisoning. Key issues include energy requirements, scaling of energy cost as a function of concentration, and subsequent chemistry. Scaling has been a significant impediment to interpretation of various data, because results have been reported for a variety of concentrations, and interpretations for different conditions are as a result difficult to reconcile between the different experiments. This article presents studies of energy required for short-pulse corona decomposition of TCE in a flowing gas stream. Experiments have been carried out for air with variable humidity and nitrogen-oxygen mixtures with variable oxygen content over a wide range, 100-2500 ppm, of initial TCE concentrations. The dependence of optimum oxygen content on the initial TCE concentration was found to be nearly linear, changing from 0.5% to 2.5% for 200 and 2000 ppm correspondingly, demonstrating feasibility of a linear dependence, and hence this aspect of the technology. The energy cost at optimum oxygen content differed by factors of 2.5 to 12 times (depending on the initial TCE concentration) than at standard atmospheric (21%) oxygen content, suggesting that the energy cost will be less if nitrogen is added to the gas stream. In this paper we report results that allow comparison for various flows, and provide a more general basis for scaling over the range of concentrations. The data reported here provide a more uniform basis for judging different conditions and concentrations. A variety of the electrical discharge reactors, as well as electron beam technologies [1,2], have been investigated for TCE removal including silent discharge [3,4], surface discharge [5], pulsed corona [4] and microwave [6] discharge techniques. It is difficult to deduce scaling laws from

these studies due to the ranges in initial TCE concentrations and variable experimental conditions — typically results are reported for a specific concentration. For these reasons this study of TCE treatment under consistent experimental conditions for a wide range of TCE concentrations and gas mixture conditions (oxygen content and humidity) was initiated, and the results are reported here. Comparison of treatment results in Ar, N_2, and N_2-O_2 mixtures enabled us to make reasonable conclusions about reactions chemistry.

2. Experimental setup

Experiments were performed in a flow-through configuration with gas flow rates 5-20 l/min using a standard commercial mass-flow controller at STP (23°C and 1 atm). TCE was produced by volatilization from the liquid state. The TCE concentration measurements and byproducts analysis was done by gas chromatograph (GC) with set of detectors (flame ionization, electron capture, nitrogen-phosphorus detectors) and mass spectrometer. Initial calibration was provided for TCE for the range 100-3000 ppm. The stability of calibration standards was about 5%. The pulsed corona reactor includes a 3 mm diameter threaded wire cathode within a 40 mm diameter, 300 mm long cylindrical anode, both stainless steel. A thyrotron-based pulse generator supplied voltage pulses to 35 kV, pulse duration 50 ns FWHM, rise time about 20 ns and pulse repetition rate up to 1 kHz. Voltage and current were monitored continuously and recorded with a fast digital oscilloscope. Energy deposition into the gas was obtained by voltage current product integration measured at the reactor. This integration was taken over times much longer than the main pulse in order to take into account pulse reflections from the unmatched load, producing a 20-100 percent increase in values of the deposited energy depending on the regime in comparison with integration done only over the main pulse duration.

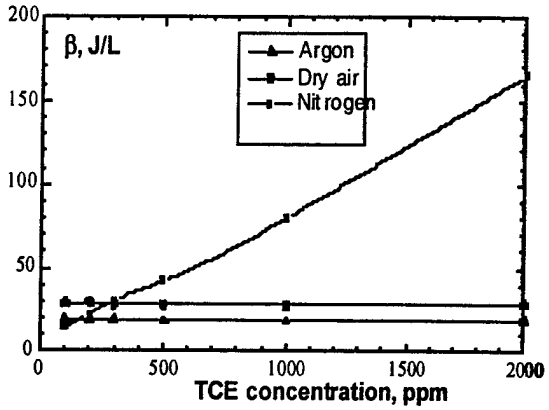

Solid State-Based Pulse Generator

A portion of the research addressed the development of improved pulsed power technologies for these applications. Improved pulsed power is a basic issue because in order to use it, the pulsed power generator must be reliable, operate repetitively for long times, and, for most applications, would be advantaged using solid state in place of gas phase switches. Research issues for solid state replacement are substantial – it is not straightforward to replace a gas-phase switch, such as a hydrogen thyratron, with solid state if the application requires pulses of the order 100 nsec, voltages in excess of 10-30kV, and current in excess of a few 10's of amperes.

Shown in the figure is a pulse generator designed and tested at USC with partial support from this project.

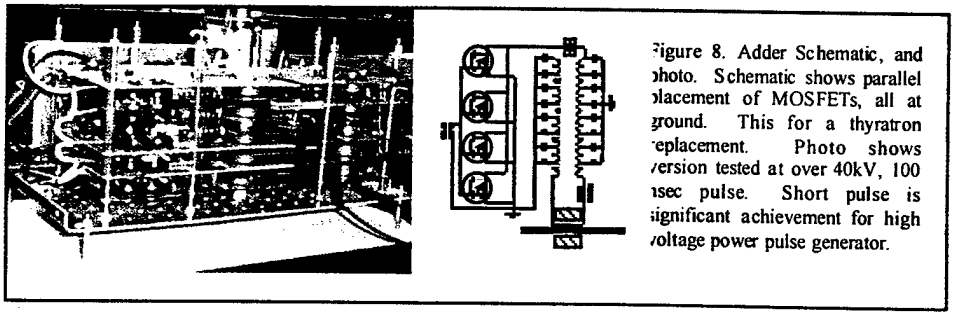

Figure 8. Adder Schematic, and photo. Schematic shows parallel placement of MOSFETs, all at ground. This for a thyratron replacement. Photo shows version tested at over 40kV, 100 nsec pulse. Short pulse is significant achievement for high voltage power pulse generator.

Shown in the figure is a schematic for a practical pulse generator called an inductive adder based on MOSFETs, and a photograph. This adder has been developed at USC as a thyrtron replacement to be used in applications where a thyratron is not practical, and it produces over 40kV with a 100 nsec pulse width. Immediately apparent is the advantage of having all input switches based at ground, reducing complexity of triggering, and alleviating the issue of series connections of the switches, which is a major issue for compact, portable systems.

3. Experimental Results and discussion

Figure 1 shows dependence of the TCE removal efficiency factor β (energy needed to remove 90% of the initial TCE) on the initial TCE concentration. While in Ar and dry air this factor is almost independent on concentration, it reveals linear increasing with concentration in nitrogen. This is indication of pseudo-first order reactions in case of Ar and air and different mechanism for N2. There is also nonlinear dependence β on concentration in N_2-O_2 mixtures at low oxygen percentage. We will consider these cases separately.

There are two possible pathways for the TCE decomposition by plasma in N_2: Dissociative electron attachment

$$C_2HCl_3 + e \Rightarrow \cdot C_2HCl_2 + Cl^- \qquad (1)$$

Reactions with nitrogen radicals

$$C_2HCl_3\ C_2HCl_3 + N \Rightarrow \text{Products} \qquad (2)$$

oxygen either in the nitrogen supply or on the

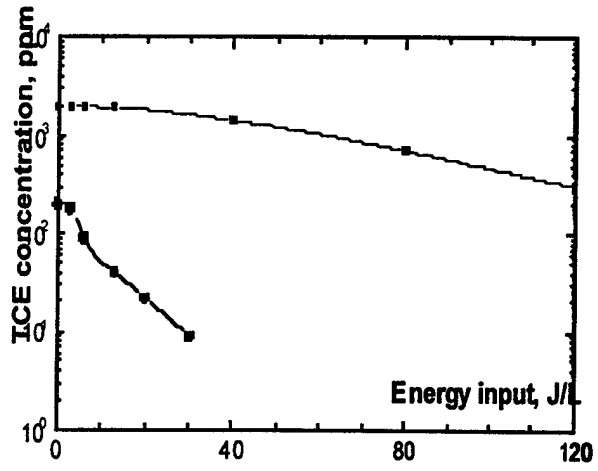

Fig. 1 Energy density required for 90% TCE removal vs initial TCE concentration.

he undesirable presence of a small amount of reactor walls due to absorption can initiate reactions by oxygen radicals. It was observed earlier [7] for example that in the surface discharge plasma treatment of CFC-113 ($C_2Cl_3F_3$) the amount of CClFO formed in the nitrogen discharge was about 10% of that in air. No analysis or discussion of this effect was presented, but it is possible to suggest that the reactor walls (made from alumina ceramic Al_2O_3) provided some amount of oxygen radicals during discharge. This example illustrates that extreme care should be taken in evaluation of experimental conditions. It was common point that the first reaction is dominant because the attachment cross section is fairly large ($1.8\text{-}3*10^{-16}cm^2$ for electron energies between 0.2-1 eV according to [8]) which corresponds to a reaction rate of $\approx 3\text{-}5*10^{-9}$ cm^3/s.

In our experiments no detectable oxygen containing species were found by mass spectroscopy after TCE treatment in nitrogen. The major byproducts identified by GC-MS spectra are CClN (cyanogen chloride) and C_2HNCl_2 (dichloroacetonitrile), and small amounts of HCl, HCN, CHCl3 and CCl4 were also detected. The byproduct composition corresponds mainly to species obtained through reaction (2). Figure 2 shows behavior of the TCE concentration vs input energy. The decay exhibits nonexponential behavior up to some threshold energy and this threshold is nearly proportional to the initial TCE concentration. This suggest that reaction (2) is occurring because an attachment process where an electron from Cl^- eventually releases with essentially same energy the process should exhibit pseudo-first character with strict exponential decay.

An analysis of byproducts and removal dependence on the energy is not sufficient to distinguish between reactions (1) and (2). It has been found in investigations of the attachment process [9] that initial formation of C_2HCl_2 radicals finally led to C_2HCl_5 (pentachloroethane), but in plasma this

Fig. 2 Exhaust TCE concentration vs input energy density in nitrogen for 200 (circles) and 2000 (squares) initial TCE concentrations.

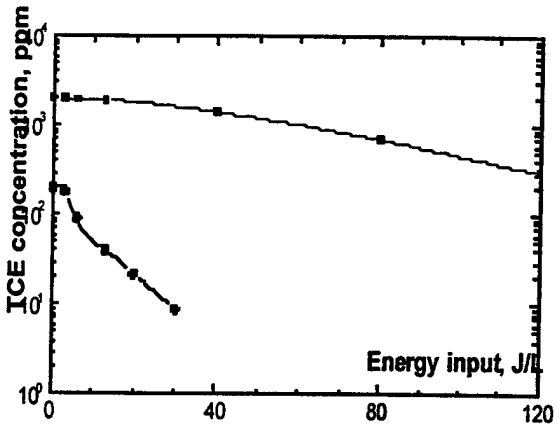

could decompose and eventually the same byproducts as for reaction (2) could be obtained. The decay behavior could deviate from exponential behavior due to reverse recombination reactions for which the reaction rate is not well defined, or loss of Cl^- through other channels. The final experiment which has been done to prove that reaction (2) is the main pathway was the addition of nitrogen oxide NO to the gas flow containing TCE. This should not influence the attachment process because only electrons with energy less than 2 eV participate (the attachment cross section drops 2 order of magnitude for energies higher than 2 eV in comparison with the maximum at 0.4 eV) but should reduce the number of N radicals because the reaction

$$N + NO \Rightarrow N_2 + O \qquad (3)$$

is fast ($3*10^{-11} cm^3/s$) in comparison with reaction (2).

These experiments revealed a strict dependence of NO addition on TCE treatment in nitrogen in that the amount of TCE removed decreased proportional to NO add. The combined experimental observations, including byproduct composition, removal efficiency vs energy input and NO influence provide strong support for reaction (2) as the dominant reaction in nitrogen.

Figure 3 shows in detail the dependence of TCE decomposition on energy input to the gas flow for three initial concentrations of TCE: 2500, 1000 and 200 ppm. The TCE removal process is observed to follow an exponential decay behavior:

$$[X]=[X_0]\exp_{10}(-E/\beta),$$

where X_0 is the initial TCE concentration and E is energy input into the gas. The most significant deviation from this behavior is at intermediate 1000 ppm concentrations, while for 100 and 2500 ppm the exponential fit is very good. This deviation is not due to experimental error because each point on this graph is an average of 5 measurements, and the accuracy of the TCE measurements and calibration

standards are at the level of 5 percent. The slope of the curves characterizes energy input required to remove 90% of the TCE initial and varies slightly from 25 J/L to 30 J/L between 2500 and 200 ppm initial TCE concentration correspondingly. The

Fig. 3 Exhaust TCE concentration vs input energy density in dry air for 200 (triangles), 1000 (circles) and 2000 (squares) initial TCE concentrations.

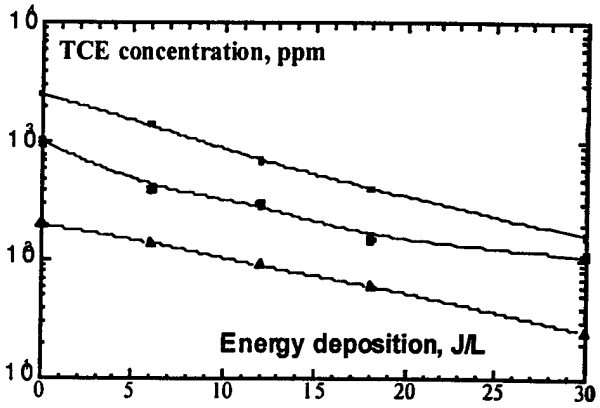

major organic byproducts identified were dichloroacetyl chloride (C_2HCl_3O, or (DCAC)) and phosgene ($COCl_2$). Trace amounts of $CHCl_3$ and CCl_4 were also detected. DCAC concentration is not linear as a function of energy input, revealing a local maximum. Due to restrictions associated with the use of DCAC and the relative instability of this product no calibration standards were utilized for this compound, so that the DCAC results are qualitative. It can be estimated roughly, though, from the peak areas that concentration of DCAC formed is substantially higher than phosgene (about 5 times).

It has been reported [9] that TCE treatment with a silent discharge in nitrogen and argon mixtures with oxygen is more efficient at low oxygen concentrations (0.3-2%) than in mixtures with oxygen at 20%, for 100 ppm TCE initial concentration, and that for a Ar-O_2 and 100 ppm TCE mixture the enhancement in efficiency is about 100 times with 0.3% oxygen content. The TCE concentration in the effluent streams of the industrial systems which use TCE as a solvent is usually quite higher, typically in the range of a few thousands ppm. To study this dependence we have carried out measurements of the TCE removal efficiency in nitrogen-oxygen mixtures at various oxygen concentrations for a wide range of initial TCE concentrations. Table 1 presents optimum oxygen percentages and β coefficient for various TCE initial concentrations.

Table 1

TCE initial concentration, ppm	Optimum Oxygen percentage	β, J/L in dry air/ and in N_2-O_2 mixture at optimum O_2 content
200	0.5	30/2.5
300	0.6-0.7	30/3
1000	1.5	27/5
2000	3	25/10

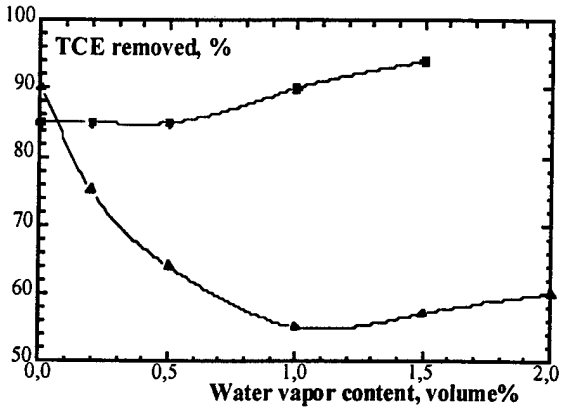

These data demonstrate that the optimum oxygen percentage increases and the efficiency enhancement coefficient decreases approximately linearly with increasing initial TCE concentration. At 2000 ppm TCE initial treatment at optimum 3% oxygen is still 2.5 times more efficient than at standard 20% oxygen content. Figure 4 shows the amount in percent of TCE removed vs oxygen content for 200 and 1000 ppm TCE at constant energy input 6 J/L. At low initial TCE concentrations the peak in efficiency is quite narrow and is broadened as the concentration increases. The oxygen content can be controlled in a reactor, so that it is possible to achieve the best reactor performance for variety of applications with different TCE content in gas streams.

The effect of humidity on the TCE decomposition has been investigated in this work for standard (80% N_2, 20% O_2 mixture). It was found [2, 3] that at concentrations lower than 500 ppm the TCE decomposition efficiency is lower in wet air. We have found, however, that the influence of humidity on the TCE removal efficiency also varies significantly with increasing TCE concentration. Figure 5 illustrates this effect. The fact that at the level of thousands ppm the decomposition process is more effective in wet air is important because water vapor is commonly present in industrial effluents. DCAC concentration decreases linearly with water content increasing both for high and low TCE concentrations.

4. Conclusion

The chemistry of TCE decomposition in gas mixtures containing oxygen is quite complicated, including hundreds of reactions with many intermediate byproducts. For many reactions there is no experimental data for reactions rates. These experiments demonstrate that there is qualitative difference in the decomposition process for the low and high TCE concentrations, and this investigation provides a set of experimental data for cold plasma TCE decomposition for a broad range of the initial concentrations that are appropriate for many practical and research situations. Optimal conditions for oxygen content and water vapor have been identified.

Fig. 4 Amount of TCE removed vs oxygen content for constant energy input 6 J/L for 200 (triangles) and 1000 ppm (circles) initial TCE concentrations.

Fig. 5 Percentage of TCE removed vs water vapor content for constant energy input 25 J/L for 100 (triangles) and 2000 ppm (circles) initial TCE concentrations.

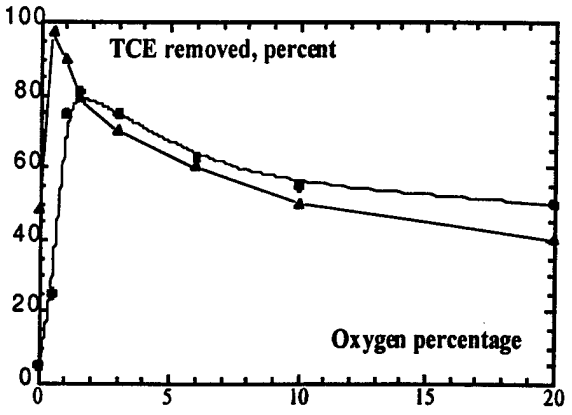

References

[1] M. Koch, D.R. Cohn, R.M. Patrick et al., Environment Science and Technology, 1995, 29, pp. 2946-52.

[2] M.G. Nickelsen, W.J. Cooper, et al., Water resourses, 1994,vol. 28, No. 5, pp. 1227-37.

[3] D. Evans, M.J. Kushner et al., J. Appl. Phys, 1993, v.74, No. 9, pp. 5378-86.

[4] M.C. Hisao, B.M. Penetrante et al., J. Appl. Phys, 1995, v. 78, No. 5, pp. 3451-56.

[5] T. Oda, T. Takahashi et al., Proc. of the 1991 IEEE Industrial Application Society Meeting, Dearborn, MI,

September 1991, pp. 734-39.

[6] L.J. Balin, M.E. Sibert et al., Environment Science and Technology, 1975, Vol. 9, p. 254.

[7] V. Puchkarev and M. Gundersen, Appl. Phys. Lett., 1997, v. 71, # 23, p. 3364.

[8] Z. Falkenstein, J.Appl.Phys., Vol. 85, No. 1, January 1999, pp. 525-29.

[9] Kwang Choo and Youn Kim, Chemical Physics Letters, 1993, Vol. 102, #2, p. 281.

[10]Rainer Kaufel et al, Chemical Physics Letters,1984, Vol. 106, #4, p. 342

Appendix 2: Premixed flame ignition by pulsed transient plasma, or corona

A flame ignition method based on pulsed corona discharges was investigated. A pulsed corona discharge is the transient phase of electric discharge before arc formation, and differs from conventional spark discharges in that the pulsed corona discharge has (1) spatially more extensive distribution of plasma species than typical sparks; (2) higher fractions of electron energies which match electron excitation cross sections for dissociation and ionization energies of molecules; (3) higher energy efficiency and (4) the possibility of in-situ NOx destruction. This paper reports experimental investigations of pulsed corona ignition using various fuels including methane, propane, iso-butane, n-butane and iso-octane at both high (>1 atm.) and low (<1 atm.) pressure regions with varying electrode structures. Experimental results show that compared with conventional spark ignition, flame ignited with pulsed corona discharges have faster (typically by a factor of 3) pressure rise time, shorter delay time, higher maximum pressure and more complete combustion. Potential applications such as improving thermal efficiency and lowering pollutant emission of internal combustion engines, high altitude relight of jet engines, flame holding in high-velocity jets, etc., are discussed.

Introduction

. Pulsed corona discharge is the transient phase of pulsed electric discharge before arc formation (1,2). Typically, corona discharge occurs in an electric field with high electric field strength gradient created by electrodes of point-plate or wire-cylinder structures. The pulse width is typically 10s ns. Under such temporal and spatial arrangements, the pulsed corona discharge has different characteristics compared with conventional spark discharge. Pulsed corona discharge usually occurs via many (e.g.10s or 100s) channels simultaneously instead of a single channel as usually spark discharge do. Therefore flame ignition with pulsed corona discharge could have more extensive spatial distribution compared with conventional spark ignition. Typically, electron energy of pulsed corona discharge is 10eV. Compare to 1eV average electron energy of spark discharge, electron energy level of pulsed corona discharge is closer to the ionization and dissociation energy levels of many combustion related species (e.g. the dissociation energy of O_2 is 9.6eV). Ions and neutral molecules in pulsed corona discharge are still remain in a temperature close to room temperature during corona discharge while electrons are in very high temperature (non-thermalized plasma). That is quite different from the high temperature characteristic observed in conventional spark discharge implying the ignition mechanisms might quite different between pulsed corona ignition and conventional spark ignition.

Pulsed corona has been extensively and successfully investigated as a means of reducing NOx created by internal combustion engines(3,4,5). Due to the similarity of principals and devices structures between flame ignition and pollution reduction by pulsed corona discharges, It is reasonable to expect that pulsed corona flame igniter might also play a role in pollutant reduction.

The characteristics of pulsed corona discharge mentioned above are quite different from conventional spark discharge (6-10), further investigation on pulsed corona discharge ignition

both experimentally and theoretically are necessary to clarify the differences on phenomena and underlying physics between them.

Section II describes experiments and results. A discussion will be given on Section III. Section IV is potential applications. Section VI is a short conclusion.

Experiments

(a) Experimental apparatus and procedures

The corona discharge generating system (11) employed a thyratron (Triton F-211) and custom-made Blumlein transmission line to create high-voltage, short duration electric discharges. A DC power supply (Xantrex XHR600-1.7), amplifier (Direct Energy TRX-1.5k) and pulse generator (Hewlett Packard 8011A) provided the required necessary power and trigger signals. Another DC power supply (Glassman High Voltage, Series EH) supplied the pulse generator. For spark ignition tests a standard automotive ignition circuit was employed, producing pulse energy of typically 70 mJ. Discharge current and voltage were measured using pulse current transformers (Pearson Electronix 411) and custom-made high voltage dividers. Signals were recorded by digital oscilloscopes.

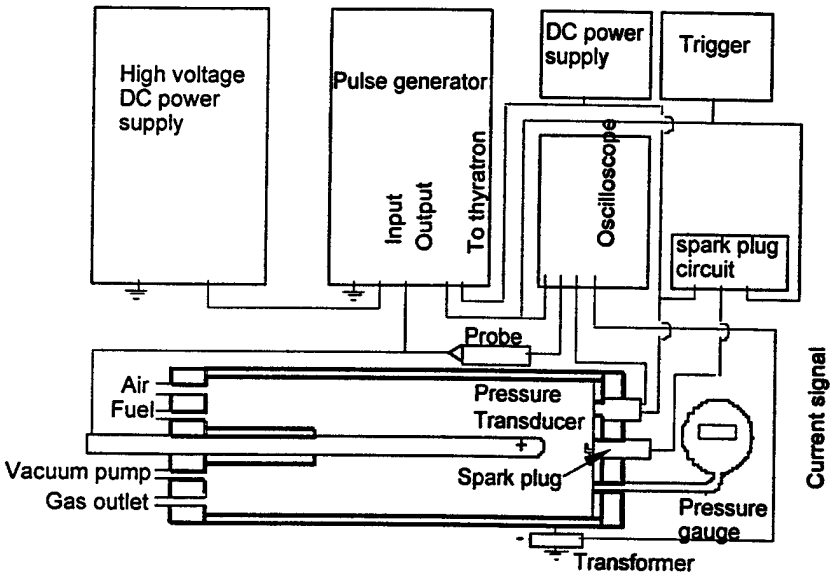

Fig.1 Experiment setup for pulsed corona ignition

The cylindrical stainless steel test cylinder dimensions were 51 mm inside diameter and 200 mm in length. This cylinder was kept at ground potential. To obtain radial-view images, in some tests this cylinder was replaced with transparent PMMA tubes lined with stainless steel screens. A 3.8 mm diameter coaxial stainless steel rod also 200 mm long served as the central electrode, creating nearly axisymmetric geometry, and was connected to high voltage. For some tests this plain rod was replaced by a "brush electrode" having 13 sets of 4 orthogonal needles spaced evenly along the length of the rod. Unless otherwise noted the central electrode was the anode (defined as positive corona polarity). One cylinder end plate had ports for gas supplies and vacuum. The other end had transducers for measuring reactant partial pressures and cylinder pressure history during combustion. To obtain axial-view images, in some tests this end plate was replaced with a transparent PMMA disk.

Two different spark locations were tested: at the cylinder end plate, using a conventional automotive spark plug (Bosch, platinum, 0.8 mm gap) and at the test chamber center using a 3mm steel rod with sharpened end nearly spanning the annulus between outer cylinder and inner rod, leaving 1 mm spark gap.

The experimental procedure was to evacuate the test chamber, fill via partial pressures, then ignite with the corona or spark discharges. Test cylinder pressure histories were recorded using digital oscilloscopes. Flame images were obtained using video and digital still cameras. Varying fuel types, equivalence ratios, pressures, corona energies and spark locations were employed to determine the most favorable operating conditions for both systems.

(b) Experimental results

i. Electrical characteristics

Figure 2 shows photographs of corona discharges without combustion. The discharges have brush-like structures with almost uniform axial (top) and azimuthal (lower left) distributions of streamers around the central electrode. For the azimuthal view, streamers were triggered at a single axial location by placing a metal disk on the central electrode. Without this disk, streamers occur along the entire length of the electrode as Figure 2 (top) shows. When the disk is replaced by four needles (Figure 2, lower right), each needle generates a tree-like streamer structure. (Figure 3 (upper left) shows an axial view of the discharge for the plain electrode (without disk)). The typical angle between streamers is 45° and the average distance between streamers along the electrode is 5 mm. Thus, there are >600 streamers in the discharge shown. This streamer distribution was mostly independent of discharge voltage; the voltage affected primarily the energy per streamer. The corona pulse energy is ~300 mJ for this case, thus the energy per streamer is ~0.5 mJ. The typical minimum ignition energy for stoichiometric hydrocarbon-air mixtures is 0.4 mJ or less [12], therefore, all of these streamers in principle could cause ignition with appropriate energy distribution within the streamer.

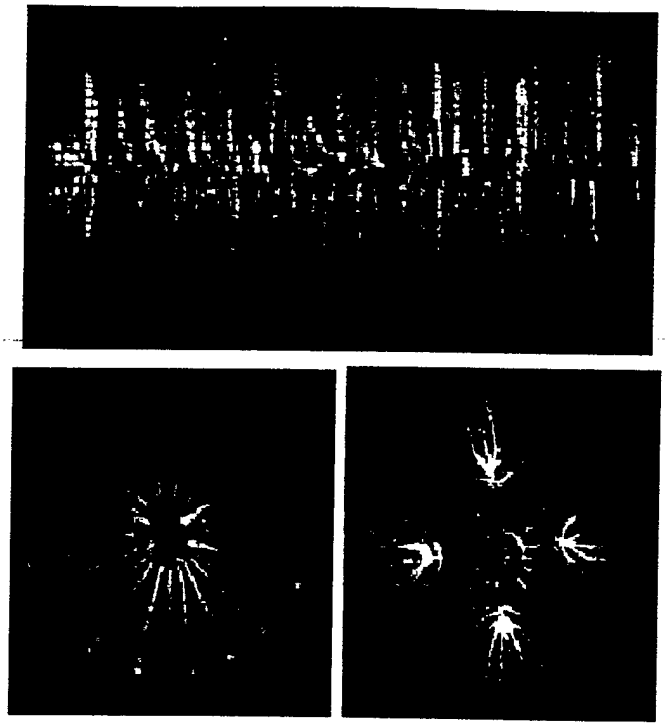

Figure 2. Images of corona discharges with plain rod electrode. Top: radial views of corona discharges air, plain electrode; lower left: axial view of corona discharge using smooth disk attached to electrode to concentrate discharge at one axial location; lower right: axial view with 4-needles attached to electrode to concentrate discharge at one axial location and 4 azimuthal locations . 300 mJ energy content in all cases. The test cell is 51 mm in diameter.

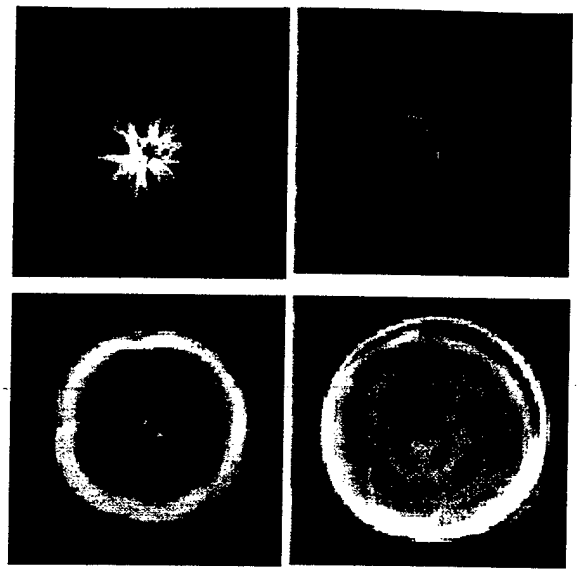

Figure 3. Sequential photographs (33 ms between images) of axial view of corona discharge ignition of a 6.5% CH4-air mixture at 1 atm, pulse energy 464 mJ, plain electrode. Chamber diameter is 51 mm.

Figure 4 (top) shows typical curves of voltage, current and integrated energy vs. time for a corona discharge. These characteristics were very repeatable and nearly independent of electrode material and gas mixture. The voltage rises to ~50 kV about 100 ns after the trigger. The current flow then begins, reaching ~190 A within ~40 ns. The current and voltage then decrease and the discharge is essentially completed within 100 ns after current began to flow. About 80% of the total energy is deposited over ~40 ns. Tests were conducted in which discharge lengths were changed by covering the part of the central electrodes with insulation. As length decreased the peak voltages were practically unchanged while the peak current decreased, resulting lower total pulse energy. Figure 4 (bottom) shows the corresponding characteristics of a corona discharge followed by electrical breakdown, obtained using slightly higher generator voltage than in Figure 4 (top). The first 100 ns are practically indistinguishable in these two cases, however, after breakdown and arc formation, the voltage drops ten-fold without corresponding increases in current, thus much less energy is deposited post-breakdown although charge from the capacitors is still consumed. Qualitatively the arc is much brighter and much noisier for the same total energy deposition. These results show quantitatively and qualitatively the decrease in energy efficiency associated with transition to arcing due to thermal and gasdynamic losses.

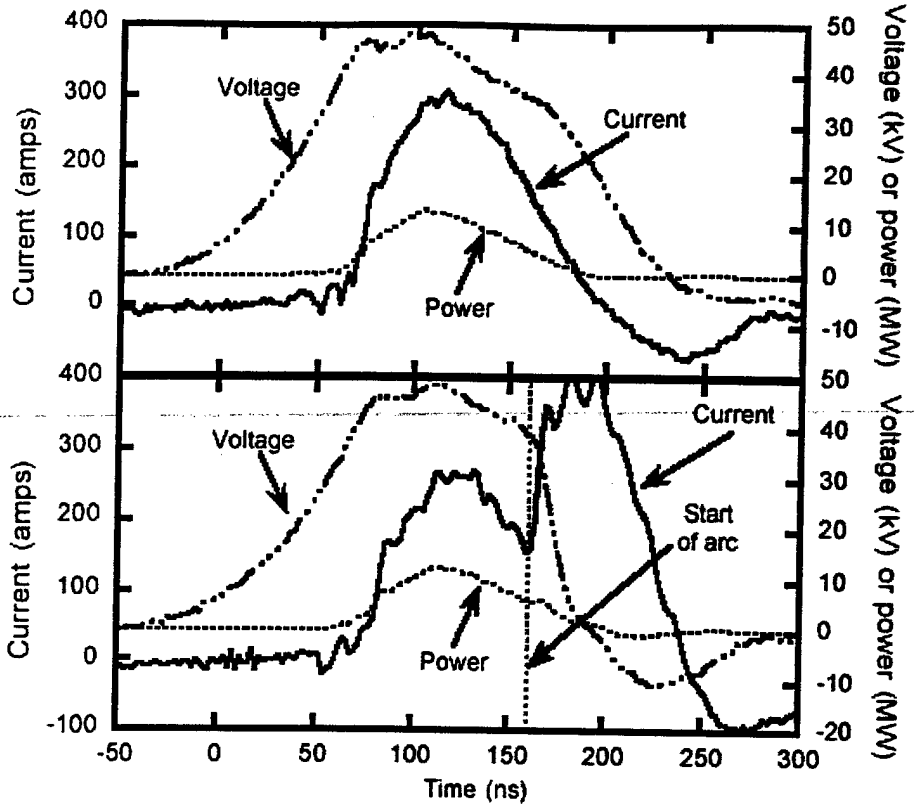

Figure 4. Voltage, current, and power vs. time for corona discharge (top) and corona with plain electrode followed by arc (bottom). Cylinder diameter 51 mm, center electrode diameter 3 mm in both cases.

It was found that no current flowed (thus no energy deposition occurred) below a threshold supply voltage. Above this threshold, energy deposition increases with increasing voltage. Thus, a particular energy deposition can be specified via the supply voltage. Smaller electrode diameters and/or the brush electrode were preferred because they provided lower thresholds and higher energy for fixed supply voltage, although the differences were minor at higher supply voltages. The 3.8 mm diameter electrode provided more than an order of magnitude range of energy deposition between the threshold (at low supply voltage) and breakdown (at high supply voltage). The brush electrode provided more than two orders of magnitude range. Positive corona polarity was found to provide higher pulse energy than negative polarity at the same supply voltage. Several combustion tests were conducted comparing positive and negative polarity at the same pulse energy (but higher supply voltage for negative polarity), with very similar results. Consequently, positive polarity was used for all subsequent ignition tests.

ii. Combustion characteristics

Figure 3 shows sequential images of a corona-ignited CH_4-air flame. The pulsed corona discharge rapidly ignites a quasi-cylindrical volume whose diameter is nearly half the chamber diameter. The ignition region surrounds the central electrode where the streamers are more densely packed.

Chamber pressure histories showed that, typical of constant-volume combustion, pressure first rises slowly then much more rapidly, then decreases very slowly after the peak due to heat losses. To compare corona and spark ignition, two combustion time scales were defined: the *delay time* (time lapse between the discharge and pressure reaching 10% of its peak) and *rise time* (duration over which pressure rises from 10% to 90% of its peak.)

Figure 5 shows the effect of corona discharge energy on rise time. An apparent "optimal" energy exists for each mixture, below which rise time increases rapidly and above which rise time is nearly constant. As might be expected, the optimal energy is higher for leaner mixtures. Delay time (not shown) decreased only moderately as corona energy increases.

Figure 6a-b shows delay time and rise time, respectively, for corona-ignited and spark-ignited CH4-air flames at varying equivalence ratios. All corona cases employed the "optimal" energy or maximum energy without arcing, whichever is lower. Figure 6a shows that corona discharges provide significant delay time reductions (about 2x) compared to the best spark location. Figure 6b shows that corona discharges provide more significant rise time reductions (by typically 3x) compared to sparks for near-stoichiometric mixtures. The differences between corona and sparks cannot be attributed to differences in energy deposition, because all ignition energies are far less than combustion heat release (~200J for stoichiometric mixtures at atmospheric pressure). These times were quite repeatable. For corona-ignited stoichiometric CH4-air mixtures the standard deviation for 6 tests was 9% and 10% of the mean value for delay and rise time, respectively. Both delay and rise times are mostly lower for brush than plain electrodes for near-stoichiometric mixtures.

Consistent with expectations based on Figure 3, generally rise time is significantly larger than delay time. Moreover, in practical combustion devices ignition delay can usually be overcome by adjusting ignition timing whereas rise times represents fundamental burning time limitations. Consequently, we focus primarily on rise time in the remainder of this work.

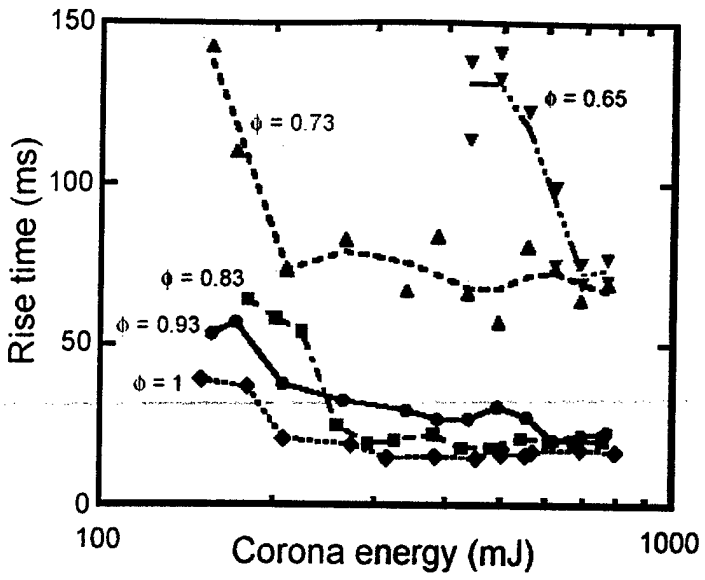

Figure 5. Rise time of corona-ignited flames as a function of discharge energy for varying values of the equivalence ratio (_) of CH4-air mixtures at 1 atm with plain electrode. The maximum corona energy shown (°800 mJ) corresponds to the threshold beyond which arcing occurs for our geometry.

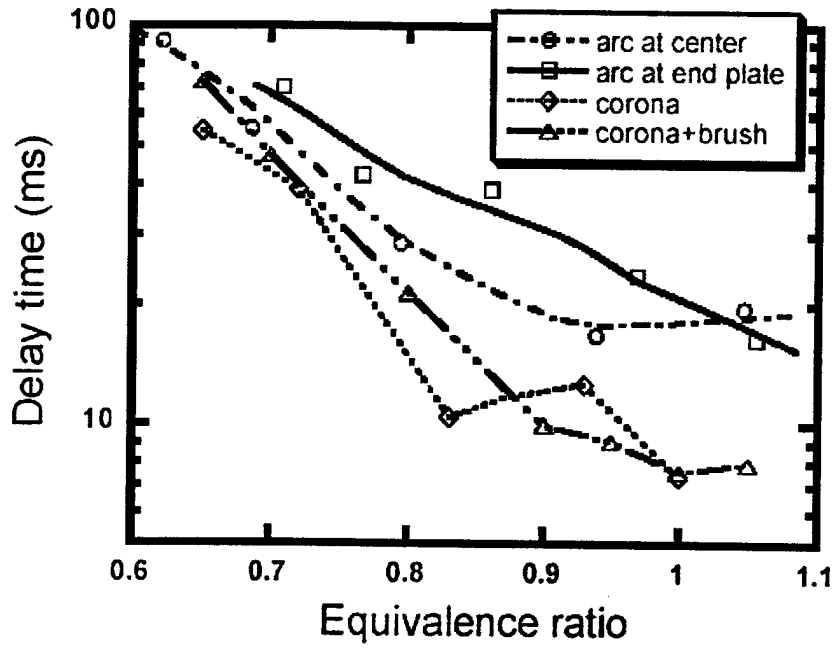

Figure 6. Characteristics of corona-ignited and arc-ignited CH4-air flames at 1 atm as a function of equivalence ratio. (a) delay time

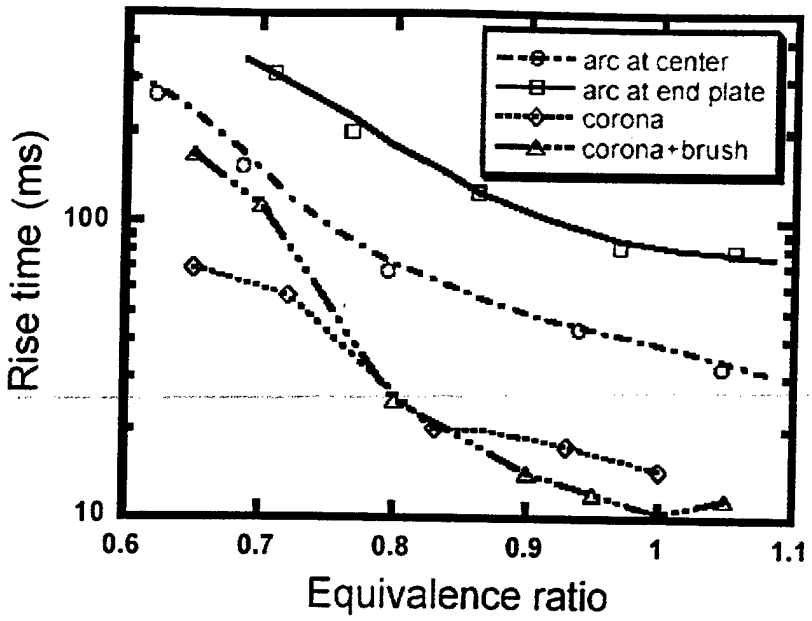

Figure 6. Characteristics of corona-ignited and arc-ignited CH4-air flames at 1 atm as a function of equivalence ratio. (b) rise time

Figure 7 shows pressure effects on rise time for propane-air mixtures. Atmospheric pressure data show trends similar to methane-air, with rise times for corona discharges still typically 3x smaller than for sparks, although the increase in rise time as equivalence ratio decreases occurs at higher equivalence ratio. For higher pressures, the advantage of corona discharges vs. sparks is maintained to lower equivalence ratios.

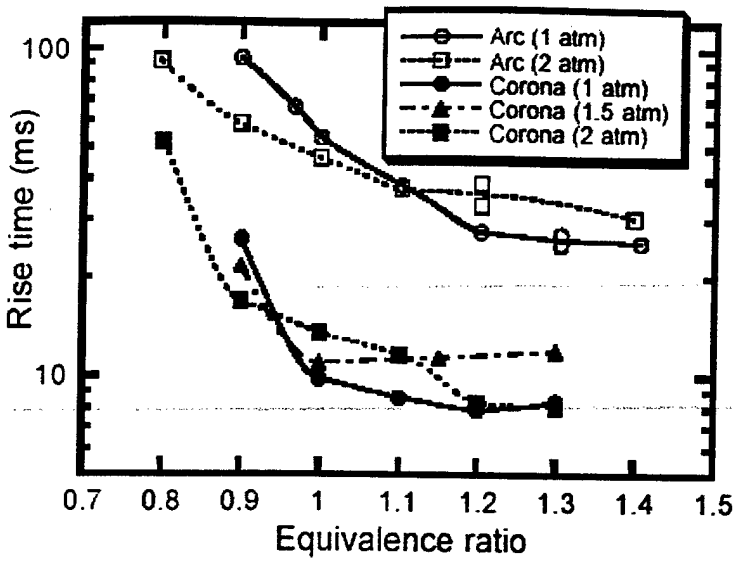

Figure 7. Rise times of corona-ignited (plain electrode) and arc-ignited (central ignition) C3H8-air flames at 1 atm as a function of equivalence ratio and pressure.

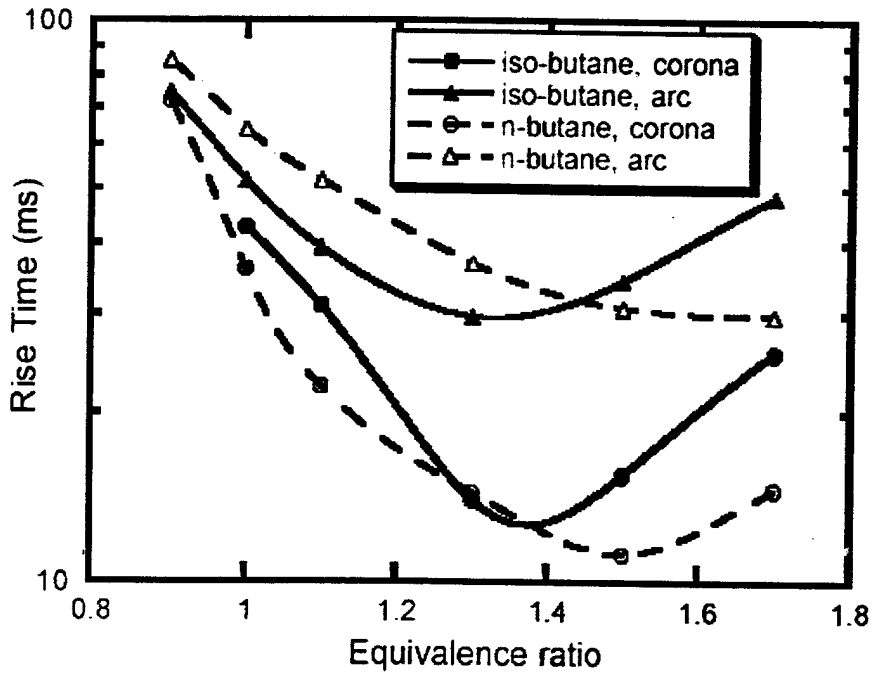

Figure 8. Rise times of corona-ignited (plain electrode) and arc-ignited (central ignition) n-C4H10-air and iso-C4H10-air flames at 1 atm as a function of equivalence ratio. Delay times (not shown) were nearly identical for all 4 cases.

To examine chemical effects, n-butane and iso-butane fuels were compared. These have nearly identical transport properties, heating values and burning velocities but n-butane has four secondary C-H bonds and no tertiary C-H bonds whereas iso-butane has no secondary C-H bonds and one tertiary C-H bond. Tertiary C-H bonds are weaker than secondary bonds, which are weaker than primary bonds; effects of bond strengths on ignition of non-ionized mixtures are well known (13). Figure 8 shows that spark and corona discharges show the same trends with changing equivalence ratio even though these trends are somewhat different for n-butane vs. iso-butane; either n-butane or iso-butane may yield lower rise times depending on equivalence ratio.

Discussion

Experiments show that corona discharge ignition provides shorter (by typically 3x) burn duration (sum of delay and rise times) than flames ignited by sparks, even at the most favorable spark location. There are at least two possible reasons: geometrical and chemical.

Geometrical advantages of corona ignition probably exist because coronas create several hundred discharge channels (Figure 2) filling the chamber volume compared to one unnecessarily intense channel for sparks. If a significant fraction of these channels produce successful ignition kernels, the distance and time each kernel must travel to consume its share of combustible mixture is greatly reduced compared to single sparks, thus delay and rise times are decreased.

Another possible advantage of corona discharges is, as mentioned earlier, the probable higher initial concentration of radicals. Computations (14, 15) show that radical sources exhibit about half the ignition delay (defined as time difference between energy deposition and virtual time origin of the steadily propagating flame) of thermal sources having the same energy input (though minimum ignition energies are similar for radical and thermal sources.) To isolate radical effects, experiments were conducted with a single-needle electrode (essentially one of four needles shown in Figure 2, lower right.) This produces more localized streamers (more reminiscent of spark discharges) than the plain corona electrode. For stoichiometric CH4-air mixtures at atmospheric pressure the delay and rise time were 22 and 26 ms, respectively, compared to 17 and 35 ms for sparks with central ignition and 7 and 15 for plain-electrode coronas. Considering that even single-needle coronas are larger than sparks, the radical effect is apparently minor since spark and single-needle corona discharges yield similar delay and rise times. Additionally, n-butane and iso-butane delay times (Figure 8) follow the trends of their respective spark comparisons . even though the trends are different for the two fuels. This also indicates miner special chemical influence of corona discharges.

The existence of .optimal. pulse energies, above which rise time is nearly independent of pulse energy and below which it is strongly dependent, could be explained as follows. As previously mentioned, the number of channels is relatively independent of pulse energy. A "minimum streamer energy" (or perhaps minimum energy per unit length) for ignition probably exists, analogous minimum ignition

energies for conventional sparks. At low energies only a fraction of these channels contain enough energy to initiate successful flame kernels. With increasing pulse energy, more channels can initiate kernels, causing shorter delay and rise times. Above some pulse energy, most channels (or perhaps a constant fraction of channels) can initiate kernels, thus further pulse energy increases have little effect on delay and rise time.

These results suggest the following simple mechanistic model of corona ignition. Corona discharges yield lower delay and rise times by creating more distributed ignition sites within the gas; chemical influences are minor. For fixed geometry, the streamer pattern is nearly independent of pulse energy. Delay and rise times are determined primarily by the fraction of streamers containing sufficient energy for ignition. With sufficient energy, delay and rise times are a surprisingly constant factor of about 3 smaller than spark discharges for our geometry. For conditions with high minimum streamer energy or where maximum discharge energy is limited by arcing, fewer kernels will ignite successful flame kernels, thus delay and rise times will increase. For very high minimum streamer energy, few kernels ignite, thus delay and rise times approach those of sparks (note corona delay and rise times approach but rarely exceed arcs.) Presumably minimum streamer energies follow the same trends as minimum ignition energies for sparks, higher for very lean or rich mixtures (12), lower pressures (12), and higher Lewis numbers (16). This simple model explains all results shown in Figs. 5-8 regarding effects of corona energy, equivalence ratio, pressure, and fuel type (Lewis numbers are approximately 0.9, 1.7 and 2.0 for lean methane-, propane- and butane-air mixtures, respectively.)

IV. Application prospect

The investigation of flame ignition by pulsed corona is still in its early stage, potential application are still far from matured. From the experimental data mentioned above, one can see that there are two properties of pulsed corona ignition that might be feasible for improving practical combustion devices.

The first one is faster burn duration. Fig.9 Shows that in the CH_4/Air and stoicheometric case, the improvement factors (defined as the ratio between rise (delay) time of spark discharge ignition to rise (delay) time of pulsed corona discharge ignition) are around 3. As equivalence ratio decreasing this two improvement factors increase. At equivalence ration equal 0.7, the improvement factors of rise time and delay time reach 5.2 and 3.6, respectively. Significantly faster burning in combustion engines might be expected if ignited by pulsed corona discharge. And the benefit might be even higher in lean fuel cases.

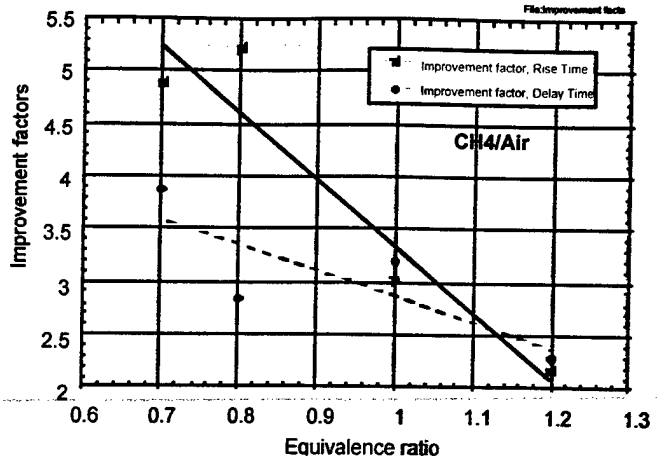

Fig.9 Improvement factors of delay time and rise time versus equivalence ratio

The second property of pulsed corona discharge ignition is the possibility of ignition at sub-atmosphere pressure conditions. Fig.10 Shows the low pressure limit of CH4/Air. In the region of equivalence ratio 0.7 to 1.0, the low pressure ignition limits are 0.1 atm. Typical pressure of high altitude relight of jet turbine engines is around 0.4-0.6 atm., therefore, pulsed corona ignition might contribute to improve high altitude relight performance of jet turbine engines.

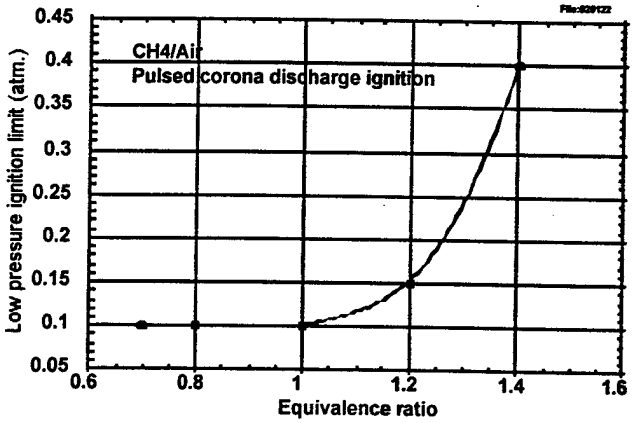

Fig.10 Low pressure limits versus equivalence ratio

There is another property of pulsed corona ignition that might also be feasible to improve practical combustion engines is the possibility of decreasing NO_x. Although we have not investigated in this area yet but that pulsed corona discharge can significantly lower NOx level in combustion engine exhaust gases is well established.(3,4,5) Due to the similarity on both principles and devices structure between flame ignition and pollution reduction by pulsed corona discharge. It is reasonable to expect that pulsed corona discharge ignition might help to decreasing pollution level of combustion engine exhaust gases.

Another important aspect in practical application is the behavior of pulsed corona discharge ignition in gases flow with high velocity and turbulence intensity. Investigation is underway and results will be published separately.

V. Conclusion

Comparison of flame ignition by pulsed corona discharges and conventional sparks shows that pulsed corona discharges have shorter (by factors of typically 3) ignition delay and rise times according to chamber pressure histories. The major advantage of coronas is apparently the spatial distribution of ignition sites, chemical effects are seemingly minor. The observed effects of discharge energy, equivalence ratio, pressure and fuel type can be explained using a simple mechanistic model considering the spatial distribution of streamers and a hypothesized minimum streamer ignition energy analogous to conventional minimum ignition energy. Comparing with conventional spark ignition, the noticeable improvements on rise and delay times and the possibilities of ignition at low pressure and NO_x removal might be helpful for improving existing combustion engines.

References

(1) Bazeluan, E.M. and Raizer, Yu.P.,"Spark discharge" CRC Press, Boca Raton, New York, 1997

(2) Creyghton,Y.L.W., "Pulsed Positive Corona Discharges" 1990

(3) Puchkarev, V., Roth, G., Gundersen, M, "Plasma processing of diesel Exhaust by pulsed corona discharge", International fall fuels and lubricants meeting and exposition, San Francisco, California, Oct. 19-22,1998, SAE technical paper series 982516

(4) Roth. G.J., Gundersen, M.A.,"Laser induced fluorescence of NO distribution after needle-plane pulsed negative corona discharge, IEEE transactions on plasma science, Vol. 27,No. 1 28-29

(5) Civitano, L., "Industral application of pulsed corona processing to flue gas",in " Non-Thermal plasma techniques for pollution control" ed . Penetrante, R.M. and Schultheis, S.E., Springer-Verlag Berlin Heidelbers, 1993, 0.3-130

(6) Maly, R., "Spark Ignition: Its Physics and Effects on the Internal Combustion Engine" in "Fuel Economy in Road Vehicles Powered by Spark Ignition Engines" ed. by Hilliard, J.C. and Springer, G.S., Plenum Press, New York and London, 1984

(7) Maly,R and Vogel, M., "Initiation and propagation of flame fronts in lean CH_4-Air mixtures by the three modes of the ignition spark, Proceeding of the 17th Symposium (Internayional) on Combustion, The Combustion Institute, Vol. 18 1747-1754, 1981

(8) Maly, R. "Ignition model for spark discharges and the early phase of flame front growth", Proceeding of the 17th Symposium (Internayional) on Combustion, The Combustion Institute, Vol. 17 821-831, 1978

(9) Davies, A.J., Davies, C.S. and Evans, C.J., "Computer Simulation of rapidly developing gaseous discharges", Proc. IEE, Vol. 118, 916-823, 1971

(10) Herweg, R.and Maly, R.R., "A fundamental model for flame kernal formation in S.I. engines", SAE paper 922 243, 1992

(11) Roth, G.J., Gundersen, M. A., *IEEE Trans. Plasma Sci.* 27:28 (1999)

(12) Lewis, B., von Elbe, G., *Combustion, Flames, and Explosions of Gases*, 3rd Ed., Academic Press, 1987.

(13) Glassman, I., *Combustion* (3rd Ed.), Academic Press, 1996.

(14). Dixon-Lewis, G., Shepard, I.G., *Proc. Combust. Inst.* 15:1483-1491 (1974).

(15). T. M. Sloane, *Combust. Sci. Tech.* 73:351-365, 1990.

(16). Tromans, P.S., Furzeland, R.M., *Proc. Combust. Inst.* 21:1891-1897 (1986).